

# JOURNAL OF ENVIRONMENTAL HYDROLOGY

*The Electronic Journal of the International Association for Environmental Hydrology*

*On the World Wide Web at <http://www.hydroweb.com>*

VOLUME 10

2002



## DERIVING LAND COVER OF A LARGE AGRICULTURAL WATERSHED FROM MULTI-TEMPORAL LANDSAT SCENES

**Samar J. Bhuyan**

Arizona Dept. of Environmental Quality, Phoenix,  
Arizona, USA

**Kyle R. Mankin**

Kansas State University, Manhattan, Kansas, USA

**J. M. Shawn Hutchinson**

**Douglas G. Goodin**

**James K. Koelliker**

---

*Determining land-cover characteristics of large watersheds for use in hydrologic models has been enhanced by application of remotely sensed data and the technologies used to interpret them. The objective of this paper was to describe and evaluate a process for obtaining land-use information for a large watershed using multi-temporal Landsat-5 Thematic Mapper (TM) images. The Kanopolis Lake watershed, which covers 6316 km<sup>2</sup> in central Kansas, USA, was evaluated. Land-cover data for 1992 was derived for use in the Agricultural NonPoint Source Pollution (AGNPS) hydrologic model. Due to shape, large size, and geographical location of this watershed, two early-summer Landsat TM images were required to cover the entire watershed. Both scenes were classified separately and then combined together to estimate land-cover information. ISODATA (Iterative Self-Organizing Data Analysis Technique) algorithm of unsupervised classification followed by supervised classification was performed. Initially, a Level-1 classification scheme was used, which differentiated cover classes among water, agricultural, rangeland, forest, residential, and barren areas. The agricultural areas were reclassified into winter wheat and summer crop and rangeland classified into low, medium, and high cover. Good agreement was found with other published land-cover spatial data, with consistent results across both Landsat scenes. Reliability, use of readily available data, and reasonable ease of use make these methods appropriate for hydrologic modeling of small to large watersheds.*

---

## INTRODUCTION

The prediction capabilities of hydrologic models depend primarily on accurate representation of the watershed conditions, including land-cover. Reliable land-cover information, however, has always been challenging to obtain. Traditional field reconnaissance techniques are time consuming, expensive, and for large and remote watersheds often infeasible. Development of land-cover classification techniques using remotely sensed data has reduced the time and effort needed to acquire data. However, large watersheds, covered by multiple satellite images pose difficulties in the classification process because of the large amount of data and variation of pixel characteristics in different images for the same area. The classification process becomes even more difficult when using historical Landsat data without ground truth data. Therefore this paper attempted to overcome these difficulties using multi-temporal Landsat-5 Thematic Mapper (TM) scenes of a large watershed to derive a land-cover map that can be used in a hydrologic model.

A GIS interface, AGNPS–Arc Info developed by Liao and Tim (1997), accepts information from GIS coverages including land-cover, soil, stream, and digital elevation, to extract parameters for the AGNPS input file. Satellite images have been used successfully to generate land-cover coverages for this model interface (Bhuyan et al., 2000). Several other hydrologic models have successfully utilized satellite imagery. Yin and Williams (1997) studied the incorporation of Landsat and AVHRR (Advanced High-Resolution Radiometer) satellite images into the crop-growth model of SWRRB (Arnold et al., 1990) to monitor hydrologic processes of a watershed. The modeled monthly runoff rates were in good agreement with the observed monthly rates. Cruise and Miller (1993) acquired spectral images using the CAMS (Calibrated Airborne Multispectral Scanner) radiance data to classify land-cover in the Rosario watershed of Puerto Rico. Land-cover data was used with Groundwater Loading Effects of Agricultural Management Systems (GLEAMS; Knisel et al., 1993) model to simulate 4 years of sediment discharge from a watershed. Cruise and Miller (1994) also used the airborne spectral images, as mentioned above, to generate input for Chemicals, Runoff and Erosion from Agricultural Management Systems (CREAMS; Knisel, 1980) model to predict runoff and sediment from a watershed.

The process of classifying satellite images is critical to the quality of land-cover data extracted. However, published descriptions often lack sufficient detail to allow recreation of the classification process for other watersheds. Furthermore, studies of watersheds that span multiple satellite images may pose additional difficulties in maintaining consistent land-cover classification across images. Therefore, the objectives of this study were to describe the steps involved in Level-1 land-cover classification of Landsat TM and demonstrate further classification of cropland into crop classes and rangeland into classes based on rangeland quality, and to verify the accuracy of developed land-cover maps.

## MATERIALS AND METHODS

This study will assess land-cover in the Kanopolis Lake watershed, which encompasses 11 counties and drains into Kanopolis Lake in central Kansas (Figure 1). The watershed includes 6,540 km of intermittent streams and 844 km of perennial streams. Kanopolis Lake watershed falls in the Central Statistics District out of nine agricultural districts of Kansas (Kansas Agricultural Statistics Service, 1996). Watershed soils are mostly silty loam and land-cover is dominated by cropland and pasture. Recently, the Kansas Department of Health and Environment initiated an assessment of the Kanopolis Lake watershed because of growing concern about overloading of sediment and nutrients

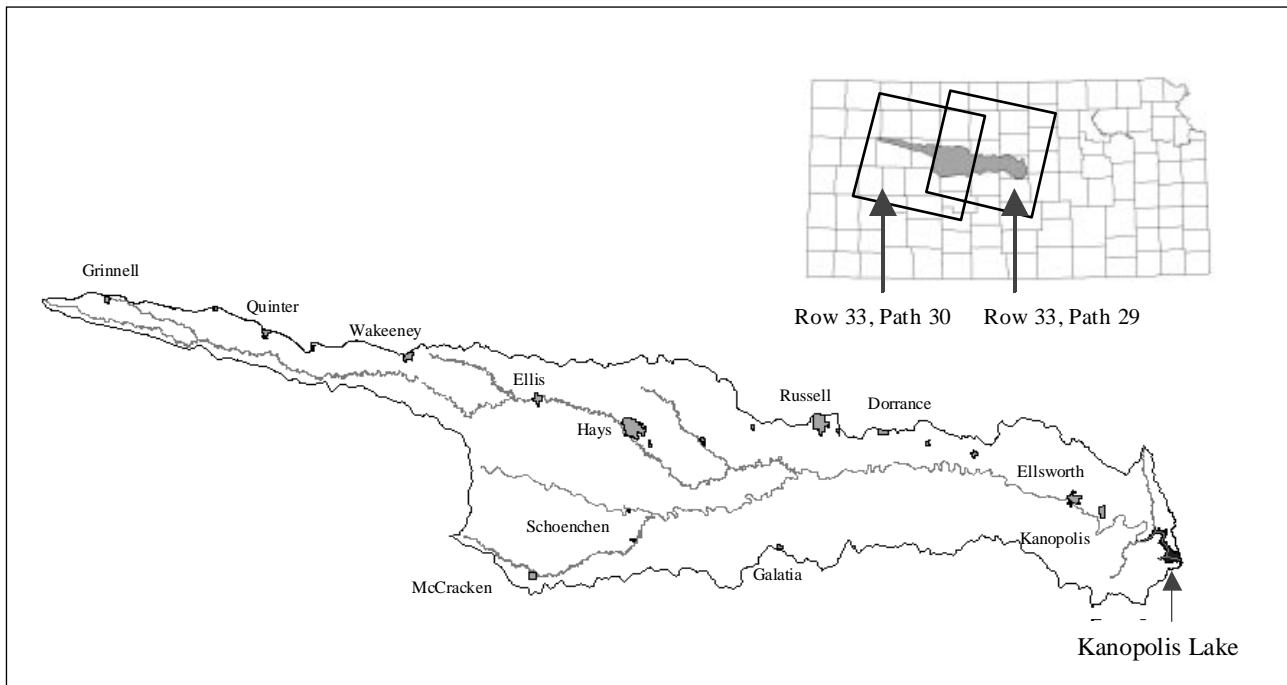


Figure 1. Location of Kanopolis Lake watershed and relevant Landsat images.

in Kanopolis Lake, a drinking water source for the City of Ellsworth and surrounding communities. The overall scope of this project is to evaluate the effects of current and potential future watershed land management on water quality.

The event-based watershed model AGNPS (Young et al., 1987, 1989, 1994) version 5.0 can easily be used to study the effects of changing conditions in a watershed (Tim and Jolly, 1995; Lee and White, 1992) and has also been successfully applied in other watersheds in Kansas (Koelliker and Humbert, 1989; Mankin et al., 1999; Bhuyan et al., 2000; Marzen et al., 2000). This model predicts event-based generation and transport of nonpoint source pollutants such as total suspended sediment, nitrogen, and phosphorous. Many of the model’s sensitive parameters are associated with the land-cover characteristics, making accurate land-cover data critical.

The AGNPS model is a single-event, distributed-parameter model developed by scientists and engineers at the U.S. Department of Agriculture-Agricultural Research Service (USDA-ARS; Young et al., 1987, 1989, 1994). The model accepts inputs from point sources such as feedlots and wastewater treatment plants, and routes these pollutants along with nonpoint source pollutants to estimate the overall watershed loads. The model discretizes the watershed into square cells, each of which is characterized by 22 input parameters: cell number, cell division, receiving cell number, aspect/flow direction, land-cover (C) factor, conservation practice (P) factor, surface condition constant, Natural Resources Conservation Service (NRCS) runoff curve number (CN), slope, slope shape and length, Manning’s roughness coefficient, soil erodibility (K) factor, soil texture, fertilizer indicator and availability, pesticide indicator, point source indicator, gully indicator, additional erosion, impoundment indicator, and channel indicator.

A GIS layer of the Hydrologic Unit Code 11 (HUC 11) boundaries for the State of Kansas was obtained from the GIS database of Kansas Data Access Support Center (DASC). The exact boundary of Kanopolis Lake watershed was then created/digitized by overlaying the digital raster graphics (DRG) of a 7.5-minute USGS quadrangle map, also available from DASC. The DRGs were used

to locate the ridge lines for delineation of the watershed boundary.

Due to the shape, large size, and geographical location of the watershed, two Landsat TM scenes are required to cover the entire watershed: Row 33, paths 29 and 30 (Figure 1). The dates of the cloud-free images obtained in this study were May 6, 1992 for the western part of the watershed and June 16, 1992 for the eastern part of the watershed. The images during this period would also be useful for classification of agricultural land because both summer crops and winter wheat will be present in the field.

The two Landsat TM images were geo-registered and rectified separately with the USGS 7.5-minute DRGs selecting more than 30 points using a second-order polynomial (Jensen, 1996). Universal Transverse Mercator projection with North American Datum 27 was selected. A root

mean square of less than 1 was obtained after re-sampling, which indicated that the error involved during this process would be within a pixel size of 30 m. Both images were also subjected to haze correction using Chavez Haze Correction model (Chavez, 1996).

An unsupervised classification was used to develop a set of 30 spectral categories for the two images. The ISODATA algorithm (Jensen, 1996) was employed for this purpose. An attempt was made to reclassify the spectral groups into thematic groups using a Level-1 classification system as described by Anderson et al. (1976). These classes included residential, agricultural, rangeland, water, barren, and forestland. However, there were some spectral categories that seem to belong to neither or more than one thematic classes. The good classes or confident classes were extracted from initial classification and remaining classes were subjected to another ISODATA algorithm of unsupervised classification. This process was repeated until the entire image was accurately classified (Figure 2).

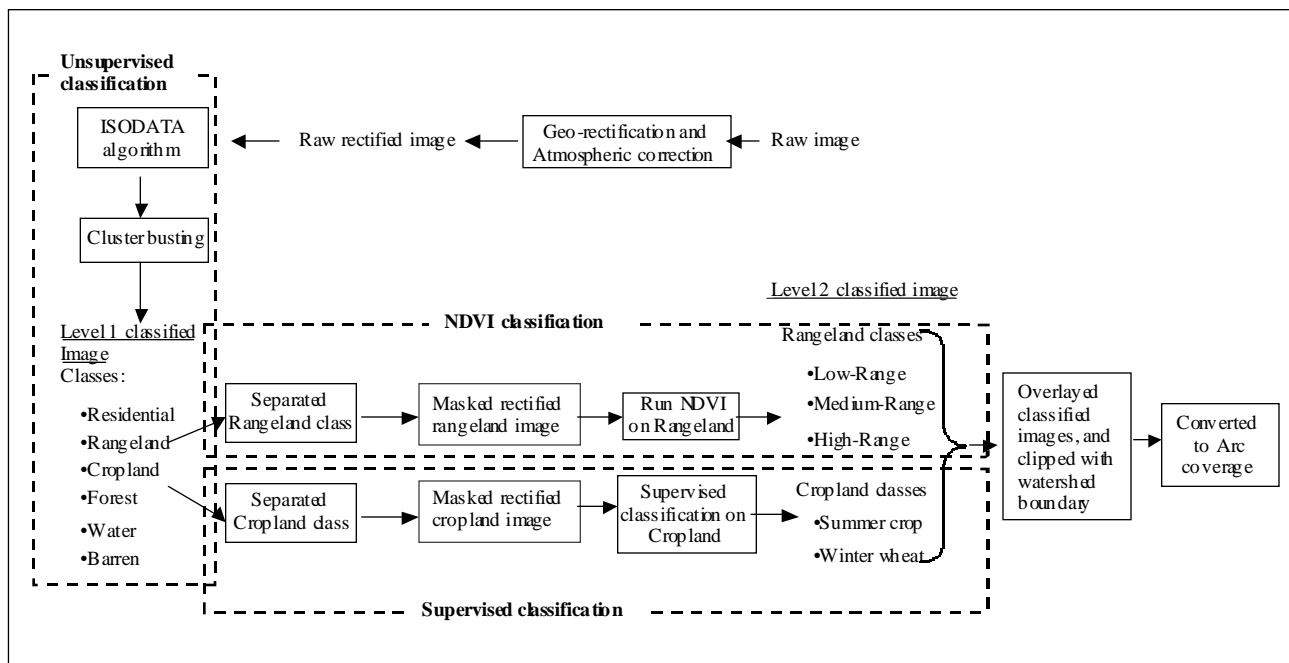


Figure 2. Schematic diagram of the land-cover classification process.

DRGs for the USGS 7.5-minute quadrangles were used for geo-rectification of the Landsat TM images. A total of 79 DRGs were obtained from DASC to cover the entire watershed. DASC also made land-cover coverages for each county of the entire state of Kansas during 1991. The land-cover

coverages for the counties located in the watershed were downloaded, joined and clipped with the watershed boundary layer, and used in the rectification and classification process. ERDAS IMAGINE 8.4 software (ERDAS Inc., 1997) was used for the classification process. The schematic view of the classification procedure is shown in Figure 2.

The next step was to sub-classify the cropland into winter wheat and summer crops (predominately corn, sorghum, and soybean) and the rangeland into low, medium, and high cover. The two major classes of cropland areas were selected as they can represent different hydrologic characteristics of watersheds. Similarly, the low, medium, and high density of rangeland would have different hydrologic impacts on the watershed. These groups differ in many parameters in the AGNPS model, including C-factor, CN, surface condition factor, and Manning's roughness coefficient (Young et al., 1994), all of which affect the runoff characteristics and the loss of sediment and nutrients from the watershed.

### **Separation of winter wheat and summer crop**

The agricultural areas of the classified images were separated and used to mask out the raw pixels of agricultural areas from the raw geo-rectified and atmospheric corrected images. The separation was done according to the recoding process described in the ERDAS IMAGINE software user manual. Supervised classification procedure was used to classify the remaining agricultural areas into either winter wheat or summer crop. Dates of satellite images were used to differentiate between winter wheat and summer crops. Based on crop-calendar reports (Kansas Agricultural Statistics Service, 1996) and expert opinion (Rogers, 2000, personal communication), it was determined that by the first week of May, winter wheat typically is in its full growing period with 100% canopy cover; corn typically has approximately 30% ground cover; and soybean and sorghum may not be planted yet or have just been planted. Usually by mid June, the winter wheat in the field is either senesced and ready to harvest or already harvested; corn is in its early growing stage; and sorghum and soybean have just been planted. Therefore, in the false-color composite, the corn would appear bright red and the winter wheat area would appear dark gray.

Some of the areas designated as cropland after the unsupervised classification had irregular field-shape characteristics and variations of spectral intensity that were indicative of rangeland. Areas designated as cropland after the unsupervised classification were separated and delineated into training areas of winter wheat, summer crop, and rangeland, and a supervised classification was performed (Jensen, 1996). The areas thus classified as rangeland were then incorporated into the other areas designated as rangeland during the unsupervised classification to create a single rangeland image.

### **Subclassification of rangeland areas**

The rangeland layer was used to mask out the pixels of rangeland areas from raw rectified images. During the period of acquiring images, the rangeland in the watershed was in its full growing season. Therefore, a Normalized Difference Vegetation Index (NDVI) was applied on rangeland pixels of the two images. The NDVI is the difference of near-infrared (TM Band 4) and visible (TM Band 3) reflectance values divided by the sum of their reflectance values (Equation (1)). The NDVI has been used to correlate with the standing green and brown biomass (Lyon et al., 1998). The value of the NDVI increases with the increasing vegetation in the scene (Malingreau, 1989).

$$\text{NDVI} = (\text{NIR band} - \text{Visible band}) / (\text{NIR band} + \text{Visible band}) \quad (1)$$

The NDVI values were rescaled from 100 to 200 to simplify analysis. The next goal was to select threshold values of NDVI to classify the rangeland areas. Due to non-availability of standard threshold values, NDVI values were divided into three equal ranges and classified as low, medium, and high vegetation density.

### **Joining the classified images**

All the classified images were combined to produce final classified images for eastern and western Landsat scenes. The final classified images had the following classes: winter wheat, summer crop, water, low-cover rangeland, medium-cover rangeland, high-cover rangeland, residential, forestland, and barren land.

An important step in the analysis of larger watersheds is joining the classified images from multiple Landsat scenes. There was a significant portion of overlapping area between the two Landsat scenes (Figure 1). Ideally, the overlapped portion in the both classified images contains the same information. However, 100% similarity is not possible due to variation of reflectance of the same objects in different images. This is attributed primarily to differences in atmospheric moisture and clouds, growth condition and moisture status of vegetation, sun angle and associated topographic shadows, and human error in the classification processes. The percent difference in the classes assigned to paired pixels could be determined using change detection techniques and then criteria developed for resolving differences. However after visual and manual cross-referencing, we found a simple overlapping operation to give satisfactory results.

During the overlapping operation, the overlapped portion of the final classified image contains the information from the image that is placed on top. We used a trial and error method to select the information from the Eastern image to represent the overlapped area. This produced a smooth overall final image with less variation of in classes along the edge of the overlapped areas and greater overall accuracy ( $P_o$ ) and Kappa coefficient of agreement ( $k$ ).

An area of interest was created from the Arc coverage of the watershed boundary, which was used to subset the classified image. Finally, a low pass (3 by 3 majority) filter was applied to reduce noise from the classified image. The raster image was then converted to a polygon coverage to use in the AGNPS–Arc Info interface model.

### **Classification accuracy**

There must be a method for quantitatively assessing classification accuracy if remote sensing-derived land-use or land-cover maps are to be useful (Meyer and Werth, 1990). Fitzpatrick-Lins (1981) suggested that the sample size  $N$  could be used to assess the accuracy of a land-use classification map using the formula for the binomial probability theory:

$$N = Z^2 p q / E^2 \quad (2)$$

where  $p$  is the expected percent accuracy,  $q = 100 - p$ ,  $E$  is the allowable error, and  $Z = 1.96$  from the standard normal deviant for the 95% 2-sided confidence level.

An expected accuracy of 85% was selected because the land-use classification system specifies that each category should be mapped to at least 85% accuracy. The allowable error of 2% was used by Fitzpatrick-Lins (1981) in a study that involved very little field verification. We used a higher allowable error of 5%, which reflects a greater level of confidence in our supervised classification process. Substituting these values into Equation (2),  $N = 196$ . IMAGINE software was used to generate a total of 205 reference points (a value  $\gg 196$  that yielded a convenient division among

classes) representing each land-cover class (Table 1).

Table 1. Numbers of Reference Points Selected from Each Land-cover Class

| Land-cover class | No. of reference points |
|------------------|-------------------------|
| 1. Residential   | 10                      |
| 2. Summer Crop   | 30                      |
| 3. Winter wheat  | 30                      |
| 4. Forestland    | 30                      |
| 5. Water         | 15                      |
| 6. Rangeland     |                         |
| Low cover        | 30                      |
| Medium cover     | 30                      |
| High cover       | 30                      |
| Total            | 205                     |

Fewer points from residential and water were selected as these two classes covered small percentages of the total watershed area. Reference-point or ground-truth data during the year 1992 were not readily available. However, DASC prepared land-cover coverages for each county in Kansas with Level-1 classification using satellite imagery and digital ortho-photography during the year 1991-1992. We have considered this data as our best estimates of independent reference data for Level-1 classification. However, the DASC coverages lumped summer-crop and winter-wheat areas into a cropland class and did not contain a barren class.

This left five classes for comparison. An error matrix was used to summarize the agreement of the current method with the baseline land-cover classification, and compute the overall accuracy of the current method. A widely used measure for estimating overall classification accuracy using an error matrix is the Kappa coefficient of agreement,  $k$  (Muller et al., 1998). The calculation of  $k$  attempts to remove chance agreement from estimates of classification accuracy by incorporating the row and column totals of the error matrix. The  $k$  coefficient is calculated from the following equation (Foody, 1992):

$$k = \frac{(Po - Pe)}{(1 - Pe)} \tag{3}$$

where  $Po$  is the observed proportion of agreement and  $Pe$  is the proportion of agreement that may be expected to occur by chance.  $Po$  is a measure of the overall accuracy and is calculated as the ratio of the number of correct classifications to the total number of comparisons made.  $Pe$  is calculated from the row and column marginals of the classification error matrix and is given by the following equation:

$$Pe = \sum_{i=1}^n Pr(i)Pc(i) \tag{4}$$

where  $n$  is the number of classes;  $Pr$  is the ratio of row marginal values to the total number of sample points and  $Pc$  is the ratio of column marginals to the total points. The range of  $k$  is 0 to 1, where greater values indicate better accuracy.

## RESULTS AND DISCUSSION

In this study, two different Landsat scenes were used to derive land-cover classes for Kanopolis watershed for the year 1992. The Level-1 classification produced 6 land-cover classes. Further breakdown of the agricultural and rangeland areas was done using supervised classification technique.

### NDVI values

The NDVI values for rangeland ranged from 106 to 174 in the western image and from 106 to 154 in the eastern image (Figure 3). This graph indicates two general characteristics of rangeland in this watershed. First, the western scene had higher frequencies for most values of NDVI and a greater overall NDVI frequency (i.e., area under the frequency curve was greater). This indicates a greater area of rangeland in the western scene than the eastern scene. Second, the distribution was shifted toward lower NDVI values (i.e., a lower mean NDVI value) in the western scene. This indicates a lower growth of rangeland vegetation in the western scene than the eastern scene. Both these

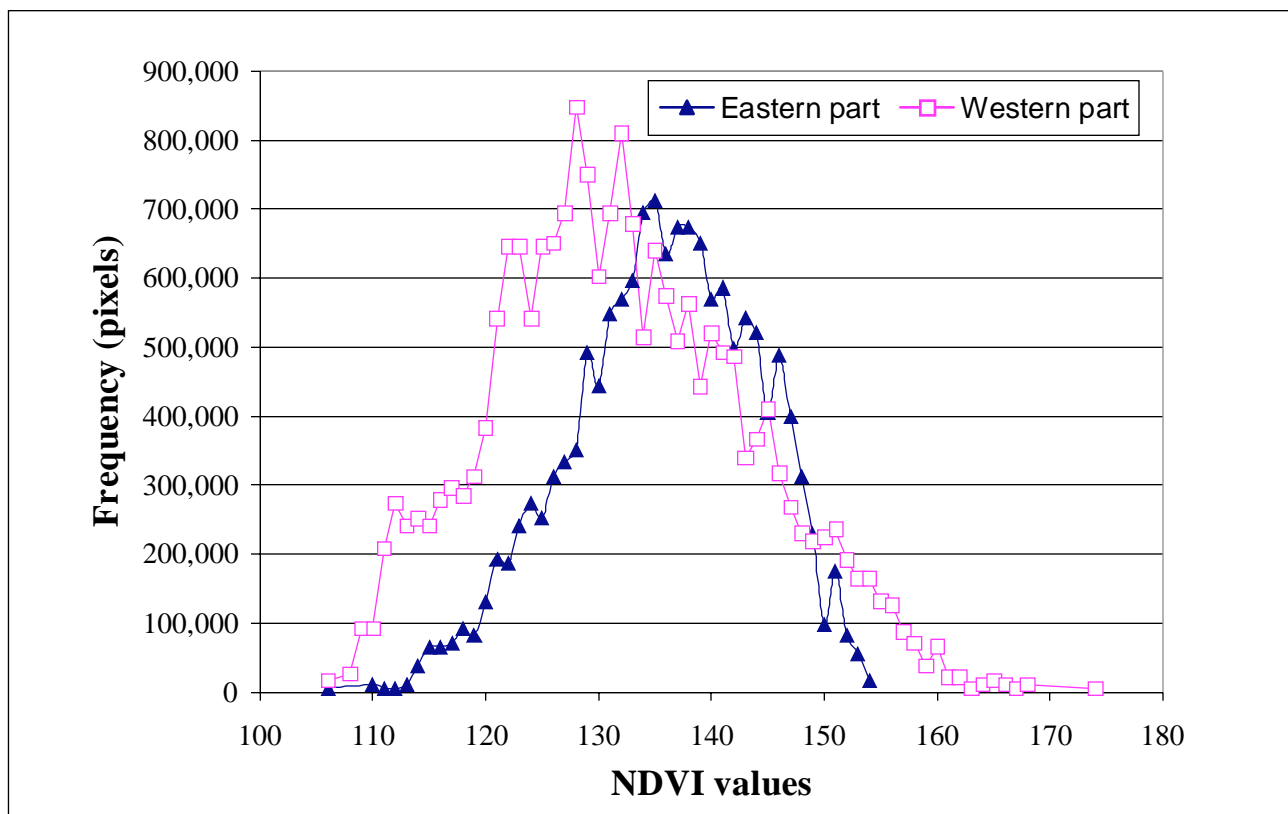


Figure 3. Distribution of NDVI values

characteristics can be explained by the distribution of rainfall and soil type in the watershed. The western part of the watershed has coarser soil texture and received less rainfall, which increased the area dedicated to rangeland instead of cropland, but also produced a lower quality of vegetation.

### Variation in land-cover

Land-cover distribution for Kanopolis Lake watershed is presented in Table 2 and Figure 4. Cropland covered 47% of the watershed and rangeland covered 52%. More rangeland area occurred in the western part of this watershed. The cropland areas could be separated into summer crops and winter wheat. In most cases the large water bodies could also be classified. However, water

classifications did not appear along the river mainstem because the width was smaller than the resolution of the pixel size. Forestland or riparian land also could be classified and appeared along the main watercourse of the watershed. Similarly, the residential areas within the watershed could be classified very well, although some of the pixels might have been lost in these categories during the smoothing process.

Table 2. Areal Distribution of Land-cover Classes from Satellite Image Data for the Kanopolis Lake Watershed During 1992

| Land-cover classes | Area               |              |
|--------------------|--------------------|--------------|
|                    | (km <sup>2</sup> ) | (% of total) |
| Residential        | 11.9               | 0.2          |
| Summer crop        | 1835.0             | 29.1         |
| Winter wheat       | 1113.4             | 17.6         |
| Forestland         | 47.9               | 0.8          |
| Water              | 18.6               | 0.3          |
| Barren land        | 9.3                | 0.1          |
| Rangeland          |                    |              |
| Low cover          | 299.4              | 4.8          |
| Medium cover       | 2112.1             | 33.4         |
| High cover         | 868.4              | 13.7         |
| <b>Total</b>       | <b>6316.0</b>      | <b>100.0</b> |

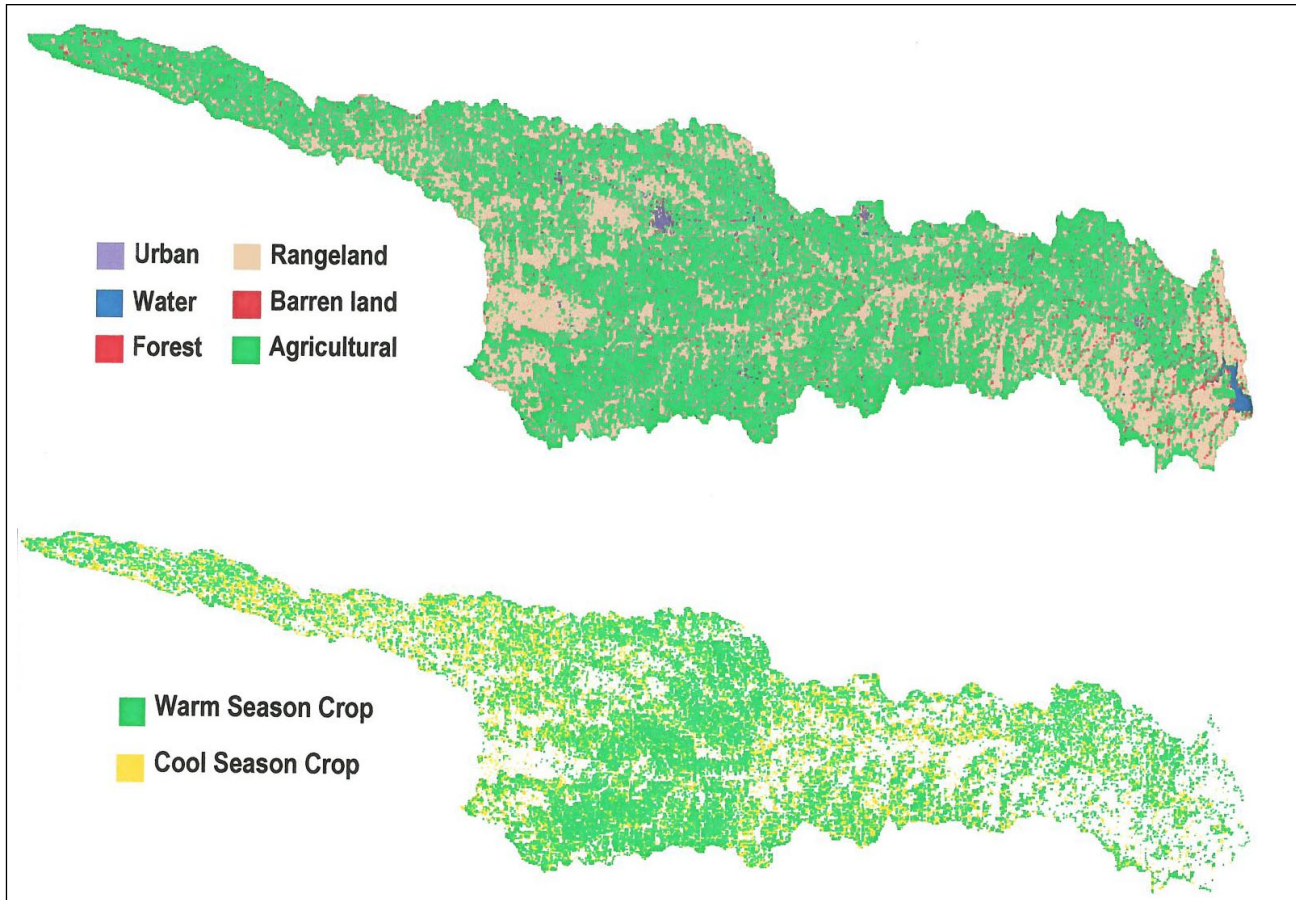


Figure 4. Classified images of the Kanopolis Lake watershed.

### Accuracy Assessment

The error matrix for five land-cover classes of residential, cropland, forestland, water, and rangeland was used to assess the accuracy of the land-cover classification (Table 3). The overall accuracy (*Po*) is the ratio of the sum of diagonal values (171) to the total number of cell counts in the matrix (205) or 83.4%. This percent accuracy is comparable to values obtained by other researchers, who reported percent accuracies ranging from 65% to 87% (Muller et al., 1998; Marsh et al., 1994; DeGloria et al., 1986).

Table 3. Error matrix comparing the classified image to the reference map.

| Landsat Classification | Reference-data Classification |          |            |       |           | Total | User's accuracy, % | <i>Pr</i> |
|------------------------|-------------------------------|----------|------------|-------|-----------|-------|--------------------|-----------|
|                        | Residential                   | Cropland | Forestland | Water | Rangeland |       |                    |           |
| Residential            | 8                             | 2        | —          | —     | —         | 10    | 80.0               | 0.05      |
| Cropland               | 1                             | 59       | —          | —     | —         | 60    | 98.3               | 0.29      |
| Forestland             | —                             | 4        | 23         | —     | 3         | 30    | 76.7               | 0.15      |
| Water                  | —                             | —        | —          | 15    | —         | 15    | 100.0              | 0.07      |
| Rangeland              | 1                             | 22       | 1          | —     | 66        | 90    | 73.3               | 0.44      |
| Total                  | 10                            | 87       | 24         | 15    | 69        | 205   |                    |           |
| Producer's Accuracy, % | 80.0                          | 67.8     | 95.8       | 100.0 | 95.7      |       |                    |           |
| <i>Pc</i>              | 0.05                          | 0.42     | 0.12       | 0.07  | 0.34      |       |                    |           |

The user's accuracy is a measure of commission errors, indicating the probability that a unit within an individual category is correctly classified; it is estimated as proportion of the diagonal value to the row total. For example, user's accuracy was  $59/60 = 98.3\%$  for cropland and  $66/90 = 73.3\%$  for rangeland. Producer's accuracy is a measure of omission errors, indicating the probability that a reference data point is correctly classified, and it is estimated as the proportion of the diagonal value to the column total. For example, producer's accuracy was  $59/87 = 67.8\%$  for cropland and  $66/69 = 95.7\%$  for rangeland.

In 22 cases, points classified as cropland by the reference coverage were classified as rangeland by the current Landsat classification. This is largely responsible for the lower user's accuracy for rangeland and the lower producer's accuracy for cropland. Assuming that the reference coverage is correct, this would suggest that high-residue croplands were incorrectly classified by our classification as rangeland. However, this may also represent low-residue rangelands that were incorrectly classified as croplands in the reference classification. This would need to be resolved using actual ground-truth data for the year in question.

Both spring burning of rangelands, which causes a temporary low-residue condition, and spring overgrazing of cattle, when winter-grazed animals are at the greatest weight prior to shipping, could explain incorrect classifications in the reference data-set. In each of these cases, the dates of images used to assess land cover as well as the dates reference data are collected are critical and must correspond. Although the reference data used in this study were collected within the same year as the images used for our classification, the published land-cover data-set does not specify the exact dates that images were taken. Thus, we cannot fully judge the correspondence of the two data sets.

With chance agreement ( $Pe$ ) of 0.297 and  $Po$  of 0.834, the  $k$  coefficient of agreement (Equation (3)) was 0.76. This compared well with the value of 0.60 obtained by Marsh et al. (1994). Again, our incorrect classification of cropland as rangeland was responsible for as much as a 0.11 reduction in  $Po$  and a corresponding 0.15 reduction in  $k$ .

## CONCLUSIONS

A reliable procedure for land-cover classification of Landsat-5 TM images for a larger watershed has been described. This classification procedure was used on two historical Landsat scenes using a hybrid classification technique that employed both unsupervised as well as supervised classification algorithms. Croplands were classified as summer crop and winter wheat, and the rangeland areas were classified into categories of low, medium, and high cover. The classified images were joined, and the resulting land-use map was used to extract the land-cover information required to develop AGNPS model inputs. This procedure is applicable for many watershed models and will allow development of required hydrologic model parameters for large watersheds with reasonable ease and accuracy.

## ACKNOWLEDGMENTS

This project is in cooperation with the Kansas Department of Health and Environment – Bureau of Water. Financial assistance for this project was provided all or in part by Kansas Water Plan Funds as well as support from the Kansas Agricultural Experiment Station (Contribution No. 02-227-J). We also acknowledge the careful reviews and useful comments provided by Dr. Prasanna H. Gowda, Senior Research Associate and Adjunct Assistant Professor (GIS, Remote sensing, and Water Resources) Department of Soil, Water, and Climate, University of Minnesota, Twin Cities Campus, St. Paul, MN, and Dr. Luke Marzen, Assistant Professor, Department of Geology and Geography, Auburn University, AL. Appreciation is also extended to Mr. Eric Rodenbaugh, Associate Editor, Department of Communication, Kansas State University, Manhattan, KS.

## REFERENCES

- Anderson, J. R., E. Hardy, J. Roach, and R. Witmer, 1976. A Land-use and land-cover classification system for use with remote sensor data. Professional Paper No. 964, U.S. Geological Survey, Washington, D.C. 28pp.
- Arnold, J. G., J. R. Williams, A. D. Nicks, and N. B. Sammons. 1990. SWRRB: A basin scale simulation model for soil and water resources management. Texas A&M University Press, College Station, TX.
- Bhuyan, S. J., J. K. Koelliker, L. Marzen, and J. Harrington. 2000. Water quality assessment for Cheney Lake watershed. ASAE Paper No. 00-2197. St. Joseph, Mich.: ASAE.
- Chavez, Pat S. Jr. 1996. Image-based atmospheric corrections – revisited and improved. *Photogrammetric Engineering and Remote Sensing*. 62(9): 1025-1036.
- Cruise, J. F. and Miller, R. L. 1993. Hydrologic modeling with remotely sensed databases. *Water Resources Bulletin*. 29(6): 997-1002.
- Cruise, J. F. and Miller, R. L. 1994. Hydrologic modeling of land processes in Puerto Rico using remotely sensed data. *Water Resources Bulletin*. 30(3): 419-428.
- DeGloria, S.D., S.L. Wall, A.S. Benson, and M.L. Whiting. 1986. Monitoring conservation tillage practices using Landsat multispectral data. *Journal of Soil and Water Conservation*. 41(3): 187-190.
- Fitzpatrick-Lins, K. 1981. Comparison of sampling procedures and data analysis for a land-use and land-cover map. *Photogrammetric Engineering and Remote Sensing*. 47(3): 343-351.
- Foody G. M. 1992. On the compensation for chance agreement in image classification accuracy assessment. *Photogrammetric Engineering and Remote Sensing*. 58(10): 1459-1460.

- Jensen, J.R. 1996. *Introductory Digital Image Processing: A Remote Sensing Perspective*. Upper Saddle River, NJ: Prentice Hall.
- Kansas Agricultural Statistics Service. 1996. *Planting, development, and harvest of major Kansas Crops*. Kansas Department of Agriculture, Topeka, KS. 39pp.
- Knisel, W. G. (Editor). 1980. *CREAMS, A field-scale model for Chemical, Runoff, and Erosion from Agricultural Management Systems*. Soil Conservation Research Report No. 26, USDA, Washington, D.C. 640pp.
- Knisel, W.G., R.A. Leonard, and F.M. Davis. 1993. *GLEAMS Version 2.1 Part I: Model Documentation*. UGA-CPES-BAED, Pub. 5, Nov. 1993.
- Koelliker, J. K. and C. E. Humbert. 1989. *Applicability of AGNPS model for water quality planning*. ASAE Paper No. 89-2042. St. Joseph, Mich.: ASAE.
- Lee, M. T. and D. C. White. 1992. *Application of GIS databases and water quality modeling for agricultural nonpoint source pollution control*. Research Report 014. Water Resources Center, University of Illinois at Urbana-Champaign, Urbana, IL.
- Liao, Hsiu-Hua and U. S. Tim. 1997. *An interactive modeling environment for non-point source pollution control*. *Journal of the American Water Resources Association*. 33(3): 1-13.
- Lyon, J. G., D. Yuan, R. S. Lunetta, and C. D. Elvidge. 1998. *A change detection experiment using vegetation indices*. *Photogrammetric Engineering and Remote Sensing*. 64(2): 143-150.
- Malingreau, J. P. 1989. *The vegetation index and the study of vegetation dynamics. Applications of Remote Sensing to Agrometeorology*. 285-303.
- Mankin, K. R., J. K. Koelliker, and P. K. Kalita. 1999. *Watershed and lake water quality assessment: An integrated modeling approach*. *Journal of the American Water Resources Association*. 35(5): 1069-1080.
- Marsh, S. E., J. L. Walsh, and C. Sobrevila. 1994. *Evaluation of airborne video data for land-cover classification accuracy assessment in an isolated Brazilian forest*. *Remote Sensing of Environment*. 48(1): 61-69.
- Marzen, L., S. J. Bhuyan, J. A. Harrington, and J. K. Koelliker. 2000. *Water quality modeling in the Red Rock Creek watershed, Kansas*. *Proceeding of the Applied Geography Conferences*. 23: 175-182.
- Meyer, M. and L. Werth. 1990. *Satellite Data: Management Panacea or potential problems?* *Journal of Forestry*. 88(9): 10-13.
- Muller, S. V., D. A. Walker, F. E. Nelson, N. A. Auerbach, J. G. Bockheim, S. Guyer, and D. Sherba. 1998. *Accuracy assessment of a land-cover map of the Kuparuk River Basin, Alaska: Considerations for remote regions*. *Photogrammetric Engineering and Remote Sensing*. 64(6): 619-628.
- Rogers, D. 2000. *Personal communication*, Department of Biological and Agricultural Engineering, Kansas State University, Manhattan, KS.
- Tim, U. S. and R. Jolly. 1995. *Evaluating Agricultural nonpoint-source pollution using integrated Geographic Information Systems and hydrologic/water quality model*. *Journal of Environmental Quality*. 23(1): 25-34.
- Yin, Z, and Williams, T. H. 1997. *Obtaining spatial and temporal vegetation data from Landsat MSS and AVHRR/NOAA satellite images for a hydrologic model*. *Photogrammetric Engineering and Remote Sensing*. 63(1): 69-77.
- Young, R. A., C. A. Onstad, D. D. Bosch, and W. P. Anderson. 1987. *AGNPS, Agricultural Nonpoint Source Pollution Model: A large watershed analysis tool*. Conservation Research Report 35. Agricultural Research Service, USDA, Washington, D.C. 77pp.
- Young, R. A., C. A. Onstad, D. D. Bosch, and W. P. Anderson. 1989. *AGNPS: A nonpoint-source pollution model for evaluating agricultural watersheds*. *Journal of Soil and Water Conservation*. 44(2): 168-173.
- Young, R. A., C. A. Onstad, D. D. Bosch, and W. P. Anderson. 1994. *AGNPS, Agricultural Nonpoint Source Pollution Model, Version 4.03: AGNPS User's guide*, July, 1994. U.S. Department of Agriculture-NRS-NSL, Oxford, Miss.

---

ADDRESS FOR CORRESPONDENCE

Prof. Kyle R. Mankin, Ph.D.  
Biological and Agricultural Engineering  
Kansas State University  
147 Seaton Hall  
Manhattan, KS 66506  
E-mail: kmankin@ksu.edu

---